ISSN 1674-1056
http://cpb.iphy.ac.cn
http://iopscience.iop.org/cpb
中国物理 B
Chinese Physics
中国物理
Chinese Physics B

Realization of THz dual band absorber with periodic cross-shaped graphene metamaterials

Chunzhen Fan(范春珍), Yuchen Tian(田雨宸), Peiwen Ren(任佩雯), Wei Jia(贾微)

Citation: Chin. Phys. B . 2019, 28(7): 076105. **doi:** 10.1088/1674-1056/28/7/076105
Journal homepage: http://cpb.iphy.ac.cn; http://iopscience.iop.org/cpb

What follows is a list of articles you may be interested in

Low-temperature growth of large-scale, single-crystalline graphene on Ir(111)

Hui Guo(郭辉), Hui Chen(陈辉), Yande Que(阙炎德), Qi Zheng(郑琦), Yu-Yang Zhang(张余洋), Li-Hong Bao(鲍丽宏), Li Huang(黄立), Ye-Liang Wang(王业亮), Shi-Xuan Du(杜世萱), Hong-Jun Gao(高鸿钧)
Chin. Phys. B . 2019, 28(5): 056107. **doi:** 10.1088/1674-1056/28/5/056107

Dynamically tunable optical properties in graphene-based plasmon-induced transparency metamaterials

Wei Jia(贾微), Pei-Wen Ren(任佩雯), Yu-Chen Tian(田雨宸), Chun-Zhen Fan(范春珍)
Chin. Phys. B . 2019, 28(2): 026102. **doi:** 10.1088/1674-1056/28/2/026102

Charge noise acting on graphene double quantum dots in circuit quantum electrodynamics architecture

Yan Li(李炎), Shu-Xiao Li(李舒啸), Hai-Ou Li(李海欧)dag, Guang-Wei Deng(邓光伟), Gang Cao(曹刚), Ming Xiao(肖明), Guo-Ping Guo(郭国平)
Chin. Phys. B . 2018, 27(7): 076105. **doi:** 10.1088/1674-1056/27/7/076105

Preparation of graphene oxides with different sheet sizes by temperature control

Zhe Qian(钱哲), Liang Chen(陈亮), De-Yuan Li(李德远), Bing-Quan Peng(彭兵权), Guo-Sheng Shi(石国升), Gang Xu(徐刚), Hai-Ping Fang(方海平), Ming-Hong Wu(吴明红)
Chin. Phys. B . 2017, 26(10): 106101. **doi:** 10.1088/1674-1056/26/10/106101

Controllable preparation of vertically standing graphene sheets and their wettability and supercapacitive properties

Hai-Tao Zhou(周海涛), Ning Yu(喻宁), Fei Zou(邹飞), Zhao-Hui Yao(姚朝晖), Ge Gao(高歌), Cheng-Min Shen(申承民)
Chin. Phys. B . 2016, 25(9): 096106. **doi:** 10.1088/1674-1056/25/9/096106

Realization of THz dualband absorber with periodic cross-shaped graphene metamaterials*

Chunzhen Fan(范春珍)†, Yuchen Tian(田雨宸), Peiwen Ren(任佩雯), and Wei Jia(贾微)

School of Physical Science and Engineering, Zhengzhou University, Zhengzhou 450001, *China*

(Received 24 December 2018; revised manuscript received 20 March 2019; published online 11 June 2019)

A dualband terahertz (THz) absorber including periodically distributed cross-shaped graphene arrays and a gold layer spaced by a thin dielectric layer is investigated. Numerical results reveal that the THz absorber displays two perfect absorption peaks. To elucidate the resonant behavior, the LC model is introduced to fit the spectra. Moreover, the strength and linewidth of the absorption peak can be effectively tuned with structural parameters and the relaxation time of graphene. Owing to its rotational symmetry, this THz absorber exhibits polarization insensitivity. Our designed absorber is a promising candidate in applications of tunable optical sensors and optical filters.

Keywords: dualband, terahertz absorber, graphene, polarization insensitivity

PACS: 61.48.Gh, 42.50.Gy, 42.25.Bs, 78.67.Pt **DOI:** 10.1088/1674-1056/28/7/076105

1. Introduction

The metamaterial perfect absorber (MPA) was experimentally discovered by Landy *et al.* in 2008 and has attracted extensive research interest.[1] The MPA is a kind of artificial plasmonic nanostructure that is usually composed of a periodic metallic structure on a ground plane and spaced by a dielectric layer. By carefully and reasonably designing its physical size and material parameters, it can couple with the incident electromagnetic wave to achieve perfect absorption of the electromagnetic wave in the GHz frequency band. Since their discovery, MPAs have experienced rapid development due to their applications in thermal, biomedical, chemical sensing, and other fields. The terahertz (THz) wave is located in a special area of transition from electronics to photonics. Through scale optimization, new devices based on metamaterials can also produce an effective response in the THz band. Ye *et al.* numerically demonstrated that a composite structure of a cut-wire array can be used as an effective absorber with a resonant absorption up to 99.9%.[2] Wang *et al.* designed a mechanically tunable absorber in the THz region. The resonant shift was achieved due to the geometric size of the absorber.[3] Luo presented a thermally dependent multiband THz absorber, which was comprised of a periodic array of closed metallic square ring resonators and metal bars.[4] In general, there are two ways to achieve multiband or broadband absorption of the incident light.[5,6] One method is to design multiple resonators with different sizes and then combine them together.[7,8] The other method is to stack resonators of different sizes on multiple dielectric layers.[9,10] However, the aforementioned structures are difficult to initiate in experiments because of the complicated metallic structure and high cost.[11,12]

Recently, graphene has been introduced into the design of plasmon-induced absorption devices due to its unique optical and electrical properties.[13,14] It exhibits the characteristics of electric field tunability and low propagation loss. In particular, the Fermi energy E_f of graphene can be dynamically tuned by using the external electrostatic gating.[14,15] Rasoul *et al.* achieved a frequency-tunable MPA based on graphene microribbons on a thick dielectric layer deposited on top of a reflecting metal substrate.[16] Luo *et al.* showed a periodic array of graphene nanodisks exhibiting 100% light absorption.[17] In addition, the combination of graphene wire and gold cut wire have been studied.[18] However, such a design usually embodies only singleband or narrowband absorption. Khavasi proposed a method to achieve broadband absorption with a periodic array of graphene ribbon, the normalized bandwidth absorption of which can reach up to 1.0.[19] Nonetheless, such proposed structures are polarization-dependent, which hampers their potential applications.

In this work, a cross-shaped graphene THz absorber is proposed. It can achieve THz dualband absorption. The designed structure consists of a periodically distributed cross-shaped graphene layer and a gold layer spaced by the SiO_2 dielectric layer. Interestingly, the resonant absorption peaks display polarization independence, namely, the resonant peak position remains the same under different polarization angles. The physical mechanism of the two resonant modes is revealed with the LC circuit model. The low-frequency resonant peak f_1 results from a typical dipole, and the high-frequency resonant peak f_2 shows a pair of opposite phase dipoles. Benefitting from the unique properties of graphene, the absorption of the proposed structure can be dynamically tuned through

*Project supported by the Key Science and Technology Research Project of Henan Province, China (Grant Nos. 162102210164 and 1721023100107) and the Natural Science Foundation of Henan Educational Committee, China (Grant No. 17A140002).

†Corresponding author. E-mail: chunzhen@zzu.edu.cn

© 2019 Chinese Physical Society and IOP Publishing Ltd

the Fermi energy and the intrinsic relaxation time via electrostatic gating instead of refabricating the structures. Moreover, the figure of merit (FOM) of the absorber is 15.35, which is higher than that of the same type of previous absorbers (14.55 in Ref. [20]). Due to its special tunable characteristics, our designed graphene structure is a promising candidate for applications in tunable optical filters and sensors.

2. Structure design and simulation method

The designed structure of the periodic cross-shaped graphene THz absorber is presented. Figure 1(a) displays the unit cell of graphene nanostructures on the SiO_2 dielectric spacer. Its dielectric coefficient is 3.9 and the thickness is 3.3 μm. a denotes the width of the cross-shaped graphene, which is 0.6 μm, and b denotes the length of the cross-shaped graphene, which is 2 μm. It is periodic in the x and y directions with periodicity $d = 3$ μm, as shown in Fig. 1(b). A linearly polarized plane wave light is normally incident along the z-axis and the angle of the polarization direction with respect to the x-axis is defined as θ. The ground plate is gold with a conductivity $\sigma_{\text{gold}} = 4.7 \times 10^7$ S/m, which is a perfect reflection in the frequency domain of interest. Both the transmission spectra and the field distribution are calculated by using COMSOL Multiphysics. It is a commercial software based on the finite element method. It subdivides a large system into smaller, simpler parts that are called finite elements. The simple equations that model these finite elements are then assembled into a larger system of equations that models the entire problem.[21] The solution of Maxwell's equations is used to calculate the electric and magnetic field components of each point in the grid space. With the continuity of the tangential electric field at each boundary, the parameters of the simulated space electromagnetism are all given in the space grid. In our calculation, the computation domain consists of only a unit cell with the perfectly matched layer applied to the boundaries along the propagation direction z and periodic conditions employed to the four lateral boundaries in the x and y directions.

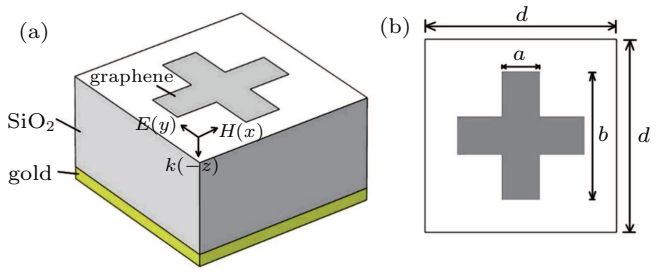


Fig. 1. Schematic view of the graphene-based dualband THz absorber. The geometrical parameters of the proposed structure are as follows: $a = 0.6$ μm, $b = 2$ μm, $d = 3$ μm, the thickness of SiO_2 is 3.3 μm, and the thickness of gold is 0.2 μm.

To carry out the simulation, graphene is modeled as a conductive surface.[18,22,23] The transition boundary condition is used for graphene, and its thickness is set as 1 nm. The conductivity of graphene can be derived within the random-phase approximation in the local limit:[17,24,25]

$$\begin{aligned}\sigma(\omega) = {} & \frac{2e^2 k_{\text{B}} T}{\pi\hbar^2}\frac{\text{i}}{\omega + \text{i}\tau^{-1}} \ln\left[2\cosh\left(\frac{E_{\text{f}}}{2k_{\text{B}}T}\right)\right] \\ & + \frac{e^2}{4\hbar}\left[\frac{1}{2} + \frac{1}{\pi}\arctan\left(\frac{\hbar\omega - 2E_{\text{f}}}{2k_{\text{B}}T}\right)\right. \\ & \left. - \frac{\text{i}}{2\pi}\ln\frac{(\hbar\omega + 2E_{\text{f}})^2}{(\hbar\omega - 2E_{\text{f}})^2 + 4(k_{\text{B}}T)^2}\right]. \end{aligned} \tag{1}$$

Here, k_{B} is the Boltzmann constant, T is the temperature, ω is the frequency of light, τ is the carrier relaxation lifetime, and E_{f} is the Fermi energy. In the calculation, our method mainly focuses on the material effect of the two-dimensional flat surface while ignoring that in the out-of-plane direction. At room temperature and low THz frequency ($E_{\text{f}} \gg k_{\text{B}}T$, $E_{\text{f}} \gg \hbar\omega$), the in-plane conductivity of the graphene can be represented by a Drude model:[26,27]

$$\sigma(\omega) = \frac{e^2 E_{\text{f}}}{\pi\hbar^2}\frac{\text{i}}{\omega + \text{i}\tau^{-1}}. \tag{2}$$

The intrinsic relaxation time is expressed as $\tau = \mu E_{\text{f}}/e v_{\text{F}}^2$, where μ is the measured carrier mobility, and $v_{\text{F}} = 10^6$ m/s is the Fermi velocity.

3. Results and discussions

The calculated absorption spectra of the cross-shaped graphene-based structure is illustrated in Fig. 2. Two perfect absorption peaks appear, corresponding to the absorption value of 96% at 6.25 THz and 97% at 14.25 THz with $E_{\text{f}} = 1.0$ eV and $\tau = 1.0$ ps. To fully determine the physical origin of the dualband THz absorber, the normalized electric field distribution and the z-component electric field distribution at the absorption peak are illustrated in Fig. 3. Figure 3(a) demonstrates that the electric field concentrates mostly on both ends of the vertical graphene ribbon, corresponding to the absorption spectra of the mode f_1 at 6.25 THz. Moreover, we can find the electric dipole resonance from the z-component electric field distribution in Fig. 3(c). Figure 3(b) shows that the electric field is mostly located around

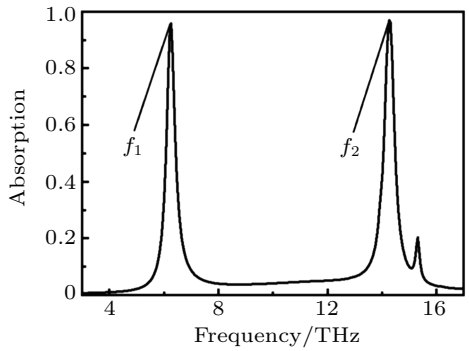


Fig. 2. The absorption spectra of the dualband THz absorber under normal incidence.

the four corners of the cross-shaped graphene, and figure 3(d) shows a pair of opposite phase dipoles that are similar to a quadrupole. Specifically, the electric fields are mainly distributed on the vertex of the graphene ribbon in the horizontal direction.

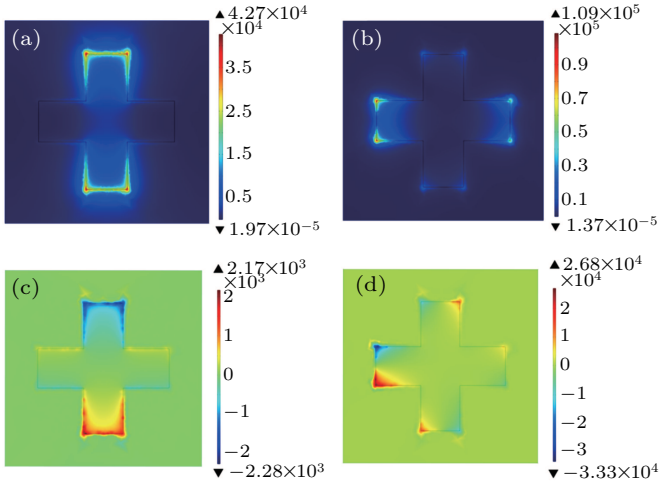


Fig. 3. The normalized electric field distribution of the dualband THz absorber at the absorption peaks (a) 6.25 THz and (b) 14.25 THz, and the z-component electric field distribution at the absorption peaks (c) 6.25 THz and (d) 14.25 THz.

In order to get a clear distribution of the resonant absorption peak position, the calculated absorption spectra of the proposed structure under different aspect ratios $a:b$ (a is taken as a constant) are shown in Fig. 4. With the decrease in length b, the peak position of the mode f_1 has a significant blue shift in Fig. 4(a). The resonant frequency of mode f_2 also increases with the decrease in length b but the degree of blue shift is much smaller than that of mode f_1 in Fig. 4(b). Employing the LC circuit model, we can gain further insight into the resonant peak position change of the f_1 mode. The resonant frequency can be obtained with the following equation:

$$f = \frac{1}{2\pi\sqrt{LC/2}} \sim \frac{1}{b}, \tag{3}$$

where C is the capacitance and it can be approximately described by a capacitor formula $C \sim (ab/2)/t$.[28] L is the inductance of the structure, which can be given as $L \sim (bt)/a$. From Eq. (3), it is clearly found that a smaller b leads to an increase in the resonant frequency of mode f_1. This agrees well with our simulation results in Fig. 4(b), namely, the resonant absorption peak shows a significant blue shift with an increase in the aspect ratio $a:b$. Because the change of the resonant mode f_2 mainly depends on the length of a, the peak position of mode f_2 is not very different from that of mode f_1.

The conductivity of the graphene layer depends to a large extent on the Fermi energy E_f, which can be tuned through the external electrostatic voltage or chemical doping. The absorption spectra of our proposed structure at different values of E_f are shown in Fig. 5. It is found that the resonant peaks move to the high-frequency region with the increase in Fermi energy. As we know, the resonant wavelength of the graphene can be given as $\gamma = \alpha + \beta \times n_g$, where α and β are constants related to the geometry parameters and surrounding dielectric properties, respectively, and n_g is the effective index of the graphene.[23,29] The effective index of the graphene layer decreases when the Fermi level changes from 0.8 eV to 1.0 eV. This results in a decrease in the resonant wavelength. Thus, an increase in the resonant frequency occurs with a larger E_f in Fig. 5.

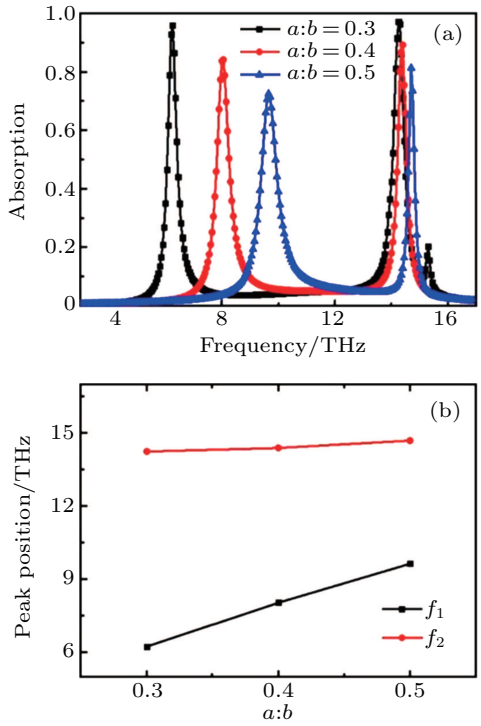


Fig. 4. (a) Absorption spectra of the dualband THz absorber with different aspect ratios $a:b = 0.3$, 0.4, and 0.5. (b) The change in peak position as a function of the aspect ratio.

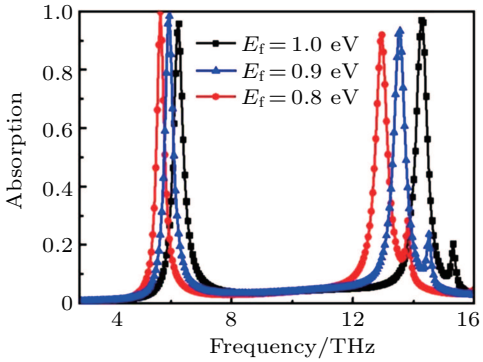


Fig. 5. Absorption spectra of our proposed dualband THz absorber with different values of Fermi level E_F.

Relaxation time τ is usually used to describe the gradual return from a certain state to an equilibrium state. It can be expressed as $\tau = \mu E_f / e v_F^2$,[30] where μ is the measured

carrier mobility, $v_F = 10^6$ m/s is the Fermi velocity, and E_f denotes the Fermi energy. Therefore, τ can be dynamically tuned by changing the Fermi energy or mobility of graphene.[31] The Fermi energy of graphene can be tuned via electrical gating or chemical doping. For gate tuning of the chemical potential, the ion gel gating method can be adopted using the field-effect transistor structure with the graphene supported by fused silica.[32–34] Thus, the electrical tunability of relaxation time in graphene can be realized in the following procedure. Firstly, a uniform graphene sheet obtained with the chemical vapor deposition method is transferred onto an ITO-coated silica substrate and then patterned into cross-shaped arrays by using electron beam lithography and oxygen plasma etching.[35,36] After patterning an array of graphene, we cover it with ion gel. A bias potential is applied between the ITO and a gold contact to electrically dope the graphene through the ion gel, which allows us to controllably tune the chemical potential over a sufficiently large range.

The absorption spectra of our proposed structure at τ in graphene elements with $E_f = 1.0$ eV are shown in Fig. 6(a). The varied intrinsic relaxation time in graphene can affect the absorption strength and linewidth of the absorption peak. The carrier mobility will be significantly enhanced when organic molecules are placed on graphene,[37] leading to an increase in relaxation time. The changes in the absorption and full width at half maximum (FWHM) at the resonant frequency as a function of the relaxation time τ are shown in Fig. 6(b). When the relaxation time ranges from 0.25 ps to 2.0 ps, the FWHM at these two resonance modes gradually decreases. In order to obtain the best absorption spectrum of graphene, a parameter Q is used to describe the relationship between the absorption intensity and the relaxation time. Q is defined as the intensity of absorption A divided by the FWHM, namely, $Q = A/\text{FWHM}$. The detailed performance of FWHM and A with different relaxation times τ is summarized in Table 1. It can be observed that the variation of FWHM and A is not consistent with the increases in relaxation time. The absorption intensity firstly increases and then decreases with increasing relaxation time. The absorbance and FWHM can be comprehensively evaluated by the parameter Q. The larger Q indicates that the absorption intensity and FWHM of the absorption spectrum have ideal values at the same time. When $\tau = 1.0$ ps, parameter Q reaches a maximum of 2.67. Therefore, we choose $\tau = 1.0$ ps to obtain the absorption spectra with higher absorption intensity and narrower FWHM.

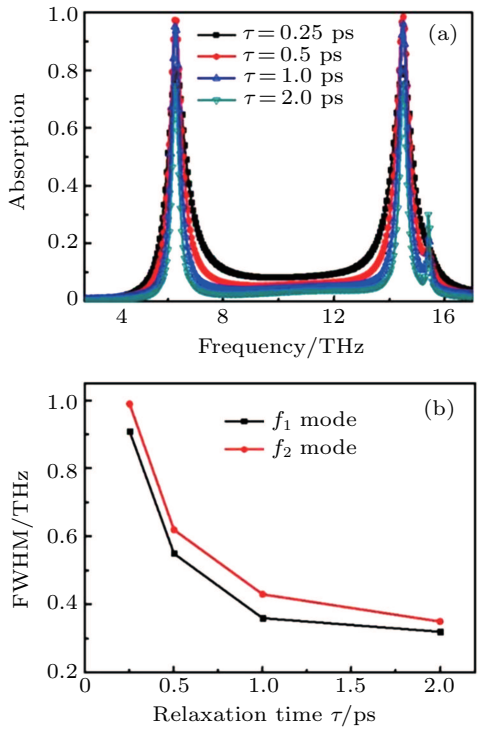


Fig. 6. (a) Absorption spectra of our proposed dualband THz absorber with different relaxation times τ. (b) The FWHM at the resonant frequency as a function of the relaxation time.

Table 1. Calculated values of parameters FWHM, A, and Q.

τ/ps	0.25			0.5			1			2		
	A	FWHM	Q	A	FWHM	Q	A	FWHM	Q	A	FWHM	Q
f_1	0.79	0.99	0.80	0.97	0.62	1.56	0.95	0.43	2.21	0.75	0.35	2.14
f_2	0.81	0.91	0.89	0.98	0.55	1.78	0.96	0.36	2.67	0.75	0.32	2.34

As an application of sensing, the absorption peak is sensitive to the variation of a nearby dielectric medium. Figure 7(a) illustrates the absorption spectra with different refractive indices of the substrate. When n is larger, the position of the absorption peak shows an obvious red shift. The refractive index sensitivity of the resonant modes can be qualified with the FOM. It can be expressed as follows:[38]

$$\text{FOM} = \frac{\Delta f}{\Delta n \cdot \text{FWHM}}, \tag{4}$$

where $\Delta f/\Delta n$ indicates the frequency shift per refractive index unit, which can be obtained from the fitted slope. Combined with the results obtained from Fig. 7(b), it is found that the FOM of f_2 can be up to 15.35, which is higher than that of the current best FOM absorber (14.55 in Ref. [39]). Therefore, the f_2 absorption peak with a high FOM can be employed in sensing applications.

The transmission spectra of the dualband THz structure under different polarization angles θ are investigated in Fig. 8. Electric field polarization angle θ is defined as the degree off the y axis. Here, θ is taken as 0°, 45°, and 90°, respectively. It can be clearly observed that the resonant absorption peaks remain stable under different polarization angles, embodying

polarization independence, which is normally due to the rotational symmetry of the unit structure.

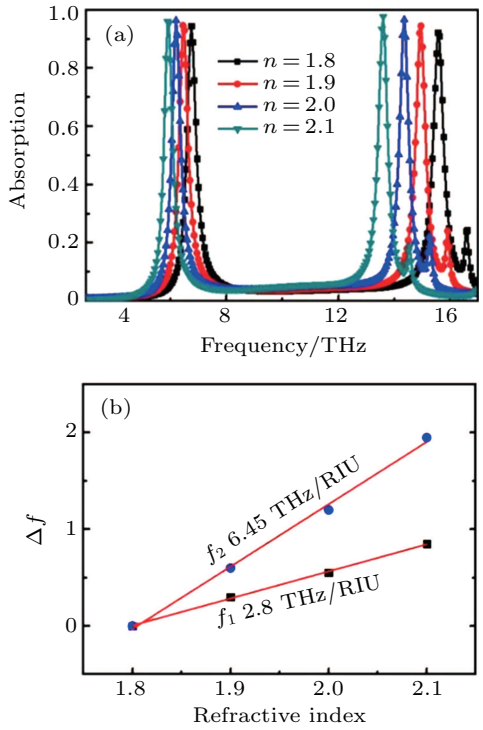


Fig. 7. (a) Absorption spectra of our proposed dualband THz absorber with different values of the refractive index n. (b) The relationship between spectral shift Δf of the absorption peak and the refractive index of the substrate.

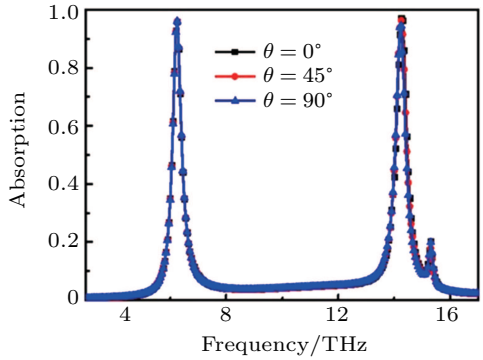


Fig. 8. Absorption spectra of our proposed dualband THz absorber under different incident angles.

4. Conclusions

In summary, we propose and numerically investigate a dualband THz absorber constructed with a graphene layer and gold film spaced by a dielectric layer. Numerical simulations indicate that two perfect absorption peaks at 6.25 THz and 14.25 THz can be realized. A simplified LC model and the electric field distribution are introduced to elucidate the resonant behavior. Our proposed absorber also embodies the polarization independency. Moreover, the absorption peaks can be dynamically tuned through the Fermi energy and the intrinsic relaxation time. With the performed sensitivity measurements, the FOM in the graphene-based structure can reach up to 15.35, which is higher than that of the same type of previous absorbers. Thus, our absorber can be used in many promising sensing applications.

References

[1] Landy N I, Sajuyigbe S and Mock J J 2008 *Phys. Rev. Lett.* **100** 207402
[2] Ye Y Q, Jin Y and He S 2010 *J. Opt. Soc. Am. B* **27** 498
[3] Wang B X, Wang L L, Wang G Z, Huang W Q, Li X F and Zhai X 2014 *J. Lightwave. Technol.* **32** 1183
[4] Luo C, Li D, Luo Q, Yue J, Gao P, Yao J and Ling F 2015 *J. Alloys Compd.* **652** 18
[5] Huang L and Chen H T 2013 *Terahertz Sci. Technol.* **6** 26
[6] Ra'Di Y, Simovski C R and Tretyakov S A 2015 *Phys. Rev. Appl.* **3** 037001
[7] Hussain S, Woo M J and Jang J H 2012 *Appl. Phys. Lett.* **101** 091103
[8] Shen X and Cui T J 2012 *J. Opt.* **14** 114012
[9] Li X, Liu H, Sun Q and Huang N 2015 *Photonics Nanostruct. Fundam. Appl.* **15** 81
[10] Liu S, Chen H and Cui T J 2015 *Appl. Phys. Lett.* **106** 151601
[11] Aydin K, Ferry V E, Briggs R M and Atwater H A 2011 *Nat. Commun.* **2** 517
[12] He J N, Wang J Q, Fan C Z and Liang E J 2015 *Opt. Express* **23** 6083
[13] Arik K, Abdollahramezani S and Khavasi A 2017 *Plasmonics* **12** 393
[14] Vakil A and Engheta N 2011 *Science* **332** 1291
[15] Fallahi A and Perruisseau-Carrier J 2012 *J. Phys. Rev. B* **86** 195408
[16] Alaee R, Farhat M, Rockstuhl C and Lederer F 2012 *Opt. Express* **20** 28017
[17] Luo X, Qiu T and Lu W 2013 *Mat. Sci. Eng. R* **74** 351
[18] Bonaccorso F, Sun Z, Hasan T and Ferrari A 2010 *Nat. Photonics* **4** 611
[19] Zhang Y, Feng Y, Zhu B, Zhao J and Jiang T 2014 *Opt. Express* **22** 22743
[20] Wang B X, Wang G Z and Sang T 2016 *J. Phys. D: Appl. Phys.* **49** 165307
[21] Logan D L 2011 *A First Course in the Finite Element Method* (6th edn.) (Boston: Cengage Learning)
[22] Thongrattanasiri S, Koppens F and de Abajo F J G 2012 *Phys. Rev. Lett.* **108** 047401
[23] Yao Y, Kats M A, Genevet P, Song N, Yu Y, Kong J and Capasso F 2013 *Nano Lett.* **13** 1257
[24] Gusynin V P, Sharapov S G and Carbotte J P 2006 *J. Phys.: Condens. Matter* **19** 026222
[25] Falkovsky L A and Pershoguba S S 2007 *Phys. Rev. B* **76** 153410
[26] Jablan M, Buljan H and Soljačić M 2009 *Phys. Rev. B* **80** 245435
[27] Hanson G W 2008 *J. Appl. Phys.* **103** 064302
[28] Zhou J, Zhang L, Tuttle G, Koschny T and Soukoulis C M 2006 *Phys. Rev. B* **73** 041101
[29] Novotny L 2007 *Phys. Rev. Lett.* **98** 266802
[30] Koppens F H L, Chang D E and Javier G D A F 2011 *Nano Lett.* **11** 3370
[31] Fu G L, Zhai X, Li H J, Xia S X and Wang L L 2016 *Plasmonics* **11** 1597
[32] Chen C F, Park C H, Boudouris B W, Horng J, Geng B, Girit C, Zettl A, Crommie M F, Segalman R A, Louie S G and Wang F 2011 *Nature* **471** 617
[33] Fang Z Y, Thongrattanasiri S, Schlather A, Liu Z, Ma L L, Wang Y M, Ajayan P M, Nordlander P, Halas N J and de Abajo F J G 2013 *ACS Nano* **7** 2388
[34] Jiang T, Huang D, Cheng J L, Fan X D, Zhang Z H, Shan Y W, Yi Y F, Dai Y Y, Shi L, Liu K H, Zeng C G, Zi J, Sipe J E, Shen Y R, Liu W T and Wu S W 2018 *Nat. Photonics* **12** 430
[35] Near R, Tabor C, Duan J and El-Sayed M 2012 *Nano Lett.* **12** 2158
[36] Chen W T, Chen C J, Wu P C, Sun S, Zhou L, Guo G Y, Hsiao C T, Yang K Y, Zheludev N I and Tsai D P 2011 *Opt. Express* **19** 12837
[37] Fang Z, Wang Y, Schlather A E, Liu Z, Ajayan P M, Javier F, de Abajo F J G, Nordlander P, Zhu X and Halas N J 2014 *Nano Lett.* **14** 299
[38] Yu X, Shi L, Han D, Zi J and Broun P V 2010 *Adv. Funct. Mater.* **20** 1910
[39] Wang B X, Wang G Z and Sang T 2016 *J. Phys. D: Appl. Phys.* **49** 165307